ELSEVIER

Journal of Molecular Catalysis A: Chemical 165 (2001) 177–188

JOURNAL OF MOLECULAR CATALYSIS A: CHEMICAL

www.elsevier.com/locate/molcata

Electrochemical behavior of lead–ruthenium oxide pyrochlore catalyst: redox characteristics in comparison with that of ruthenium dioxide

Jyh-Myng Zen*, Annamalai Senthil Kumar, Jyh-Cheng Chen

Department of Chemistry, National Chung-Hsing University, Taichung 402, Taiwan

Received 27 May 2000; accepted 22 August 2000

Abstract

The electrochemical redox behavior of lead–ruthenium oxide pyrochlore catalyst ($Pb_2Ru_{2-x}Pb_xO_{7-y}$, $x = 0.25$) was systematically studied and possible ruthenium redox species were determined by probing with formaldehyde and glucose oxidation reactions using a PVC/$Pb_2Ru_{1.75}Pb_{0.25}O_{7-y}$ composite electrode. Trasatti's surface charge formalism was applied to calculate the different accessible interfacial surface charges. Both the outer/inner and anodic/cathodic charge ratios were found very different to those of pure RuO_2 electrode. It is important to note that higher cathodic charges were noticed in all scan rates (v) and pHs for $Pb_2Ru_{1.75}Pb_{0.25}O_{7-y}$. The calculated pH_{PZC} of 3.9 from the electrochemical measurements match exactly with that of earlier titrimetric result. The electrocatalytic mediated reactions were demonstrated with $Ru^{3+/4+}$ assisted oxygen reduction reaction and $Ru^{4+/6+}$ assisted dopamine oxidation using a Nafion/$Pb_2Ru_{1.75}Pb_{0.25}O_{7-y}$ composite electrode. Rotating disk electrode technique was adopted to derive kinetics and mechanism of these two catalytic reactions.

Keywords: Lead–ruthenium oxide pyrochlore; Ruthenium dioxide; Chemically modified electrodes

1. Introduction

Ruthenium dioxide (RuO_2) is a well-known material that has been used for long as an electrode for catalyzing multi-electron transfer chlorine evolution reaction, oxygen evolution reaction (OER), and organic oxidation [1–3]. Similarly, lead–ruthenium oxide pyrochlore ($Pb_2Ru_{2-x}Pb_xO_{7-y}$) has also been used in many electrocatalytic applications [4–13]. The catalytic material possesses high surface area and is a good alternative for RuO_2, and in some cases, it is even superior to RuO_2 [7,14]. Detail investigation on $Pb_2Ru_{2-x}Pb_xO_{7-y}$ regarding its structural properties, catalytic effects, oxidative stability, and electrochemical activity with respect to different ruthenium species and the surface protonation of the pyrochlore material as a function of pH were reported earlier [7,15–19]. Based on these reports, the redox species of the pyrochlore material in aqueous solution are $Ru^{2+/3+}$, $Ru^{3+/4+}$, and $Ru^{4+/5+}$. However, it is contradictory that the reported redox species of RuO_2 in heterogeneous and aqueous solutions are $Ru^{3+/4+}$, $Ru^{4+/6+}$, and $Ru^{6+/7+}$ [1,20–35]. One of the main purposes in this study is therefore to understand and clarify the possible redox transitions in $Pb_2Ru_{1.75}Pb_{0.25}O_{7-y}$.

Both the PVC/$Pb_2Ru_{1.75}Pb_{0.25}O_{7-y}$ composite electrode (PPCE) and Nafion/$Pb_2Ru_{1.75}Pb_{0.25}O_{7-y}$

* Corresponding author. Fax: +886-4-2862547.
E-mail address: jmzen@dragon.nchu.edu.tw (J.-M. Zen).

1381-1169/01/$ – see front matter
PII: S1381-1169(00)00413-1

composite electrode (NPCE) were adopted in the present investigation. It has been established that the PVC-metal oxide composites possess highly stable and reproducible electrochemical behavior with no interference with respect to the PVC binder [29,31]. Initial electrochemical studies were done by using PVC composites with a loading amount of ~40 mg/cm^2 $Pb_2Ru_{1.75}Pb_{0.25}O_{7-y}$. The electrochemical mediated catalytic mechanisms were further demonstrated using the NPCE with a very low oxide loading. Detail electrochemical investigation was made on $Pb_2Ru_{1.75}Pb_{0.25}O_{7-y}$ regarding its redox species and interfacial surface charge effects. The interfacial surface charge with respect to the inner (q^*_{in}) and outer (q^*_{out}) active sites were calculated based on the Trasatti's surface formalism [28,29,32,33]. Standard electrochemical mediated probe reactions, namely, $Ru^{4+/6+}$ mediated oxidation of formaldehyde [34] and $Ru^{6+/7+}$ mediated oxidation of glucose [35] were performed to assess the participation of higher oxidation ruthenium redox species in $Pb_2Ru_{1.75}Pb_{0.25}O_{7-y}$.

2. Experimental

2.1. Reagents

Polyvinyl chloride (inherent viscosity = 0.8), Nafion perfluorinated ion-exchange powder, 5 wt.% solution in a mixture of lower aliphatic alcohols and 10% water, and Nafion 117 were obtained from Aldrich (Milwaukee, WI, USA). Lead nitrate ($Pb(NO_3)_2$), ruthenium chloride ($RuCl_3{\cdot}xH_2O$), and tetrahydrofuran (THF) were also obtained from Aldrich. All the other compounds used in this work were prepared from ACS-certified reagent grade chemicals without further purification in doubly distilled deionized water.

2.2. Apparatus

All voltammetry experiments were performed with the BAS-100B electrochemical analyzer (West Lafayette, IN, USA). The three-electrode system consists of either the PPCE or NPCE working electrode, an Ag/AgCl/KCl (3 M) reference electrode, and large area platinum wire counter-electrode. Since the ruthenium redox potentials are pH-dependent, in order to compare with the reported standard redox potential of ruthenium metal ions in the reversible hydrogen scale (RHE, where $E^0_{RHE} = 0$ V), the following simplified equation is used to adjust the potentials from $E_{Ag/AgCl}$ to E_{RHE}.

$$E_{RHE} = [(E_{Ag/AgCl} + 0.075 \log pH) + E^0_{Ag/AgCl}] \quad (1)$$

2.3. Preparation of high surface area $Pb_2Ru_{1.75}Pb_{0.25}O_{7-y}$ powders

The preparation of the high surface area $Pb_2Ru_{1.75}Pb_{0.25}O_{7-y}$ was described elsewhere [4]. In brief, (1:1.25) molar ratio of $RuCl_3{\cdot}3H_2O$ and $Pb(NO_3)_2$ were dissolved in aqueous solution at 75°C under constant stirring and purging of the solution with O_2 for 24 h. Approximately, 6% KOH was added to the solution so as to maintain a pH 13.5. The filtered product was washed with distilled water until any alkali present was removed. It was then annealed at 130°C for 24 h. The obtained powders are very stable with the pH_{PZC} value of 3.9 by acid–base titrimetric method [4]. X-ray powder diffraction gave broad pyrochlore peaks in an amorphous background indicating the formation of a highly porous pyrochlore material. The estimated BET surface area value was 71 m^2/g.

2.4. Preparation of the polymer-$Pb_2Ru_{1.75}Pb_{0.25}O_{7-y}$ composite electrodes

For the preparation of the PPCE, a homemade 0.5 cm height and 0.5 mm diameter Pt wire embedded glass electrode was used as the base electrode. Before coating the oxide, the Pt wire was heated in blue-flame to rod hot to remove the surface contamination. A (4:1) wt.% of $Pb_2Ru_{1.75}Pb_{0.25}O_{7-y}$ and PVC is mixed well with minimum quantity of THF [31]. Then, the PVC/oxide paste was coated onto the surface of the Pt wire and air dried at room temperature for 48 h. Note that poor adhesion of the coating to the Pt substrate can easily detected by observing the increased asymmetry in the voltammetric peaks or tilting of the voltammograms with respect to the potential axis. As to the preparation of the NPCE, ~0.02 wt.% of catalyst loaded 4% Nafion solution was coated by spin coating at 3000 rpm on a clean GCE surface with a geometric area of 0.0707 cm^2.

Both the PPCE and NPCE were preconditioned by cycling the potential between oxygen and hydrogen evolution windows in its base electrolyte solution at 50 mV/s until the voltammograms reached a constant. Then, the electrodes can be used for specific application reactions.

3. Results and discussion

3.1. Electrochemical behavior of the PPCE

Fig. 1 shows the typical cyclic voltammetry (CV) response of the PPCE between −0.2 to 1.2 V at $v = 50$ mV/s in 1 M sulfuric acid solution. Two anodic peaks at 0.65 and 0.95 V and two cathodic peaks at 0.54 and 0.91 V were observed over a large background current. Varying the switching potential in CV identified the cathodic counter parts of the anodic peaks. The $E_{1/2}$ values are 0.59 and 0.93 V (i.e. 0.81 and 1.15 V versus RHE) for the two redox couples,

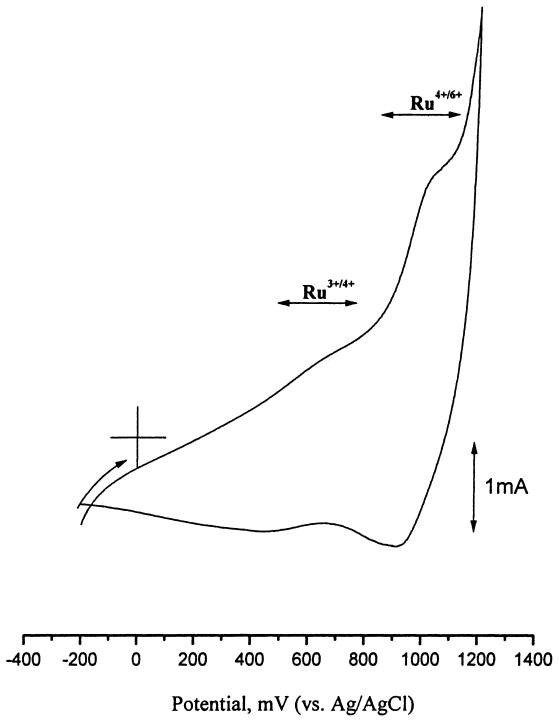

Fig. 1. Cyclic voltammogram of the PPCE in 1 M H_2SO_4 at $v = 50$ mV/s.

respectively. Interestingly, the obtained values are similar to those of RuO_2 redox behavior reported earlier [1,22,28,29,31]. Possible redox reactions exist in RuO_2 electrodes between hydrogen and oxygen evolution regions were reported earlier and summarized as follows [1,21–25,28].

$$2Ru^{4+}O_2 + 2H_2O + 2e^- \rightarrow Ru_2^{3+}O_3 + 2OH^-, \quad E = 0.4\text{–}0.5\ \text{V versus RHE} \tag{2}$$

$$Ru^{6+}O_4^{2-} + 2H_2O + 2e^- \rightarrow Ru^{4+}O_2 + 4OH^-, \quad E = 0.9\text{–}1.15\ \text{V versus RHE} \tag{3}$$

$$Ru^{7+}O_4^- + e^- \rightarrow Ru^{6+}O_4^{2-}, \quad E = 1.35\text{–}1.45\ \text{V versus RHE} \tag{4}$$

Note that the highest oxidation redox pair ($Ru^{6+/7+}$) cannot be detected in H_2SO_4 medium due to the OER at 1.1 V versus RHE. Indeed, we did not observe the $Ru^{6+/7+}$ redox pair at the PPCE, which further prevail the similar ruthenium species in $Pb_2Ru_{1.75}Pb_{0.25}O_{7-y}$ to that of RuO_2.

Similar experiments were also carried out on the PPCE in pH 4.6 acetate buffer, pH 7.4 phosphate buffer, and 1.1 M KOH and very poor redox currents were observed in all solutions. It is as expected due to the following three reasons: first, the high double layer origin of the oxide materials; second, the occurrence of H^+ or OH^- insertion reaction coupled with metal redox transition [28,31], which in turn alter the exchange ability of H^+ or OH^- ions in intermediate pHs; third, the presence of the active oxygen species (O') and the entrapment of the active ruthenium species in the interstitial sites of the pyrochlore network [4,14]. The CV responses obtained from earlier works on pyrochlore modified electrodes also showed poor redox transition signals [14]. The double layer charge for the PPCE in 1.1 M KOH solution was then measured using the small amplitude CV technique [28,29,31]. Based on the *I–V* plot, by cycling the electrode in narrow potential window of −0.4 to −0.2 V versus Ag/AgCl at different scan rates, the calculated double layer charging capacitance is 787 mF/cm^2. It is assumed that no faradic processes appear in this potential window. This result is close to 791.7 mF/cm^2 for porous and high capacitance PVC-RuO_2 (400°C) composite electrode in 1 M NaOH solution [29,31] with a similar phenomenon of no specific redox transition peaks. Taking

the reported value of 60 μF/cm^2 for porous oxide materials, the electrochemically active surface area was then calculated as 33.13 m^2/g [1,24]. This is about half to the BET surface area of 71 m^2/g. The difference is as expected since the electrochemically active surface area defines the area that are accessible in solution with fraction of the oxide surface sites and may vary from solution to gas phase. There results indicate the high accessibility to later case.

In order to understand the surface redox transitions in various pHs on the PPCE, known amount of dissolved organic compounds were added as probes and CV was performed in different pH solutions. For RuO_2, the existences of possible redox transitions were confirmed by studying the oxidation of benzaldehyde (oxidative mediation by $Ru^{4+/6+}$ redox transition) [22], benzyl alcohol ($Ru^{6+/7+}$ transition) [22], and glucose ($Ru^{6+/7+}$ transition) [35]. Similar experiments were thus applied to the PPCE using formaldehyde and glucose as probes. Since the mediated oxidation peaks are improper neither at very slow nor at fast scan rates, the experiments were carried out at $v = 50$ mV/s in wide pH windows. As illustrated in Fig. 2, the oxidation of formaldehyde and glucose

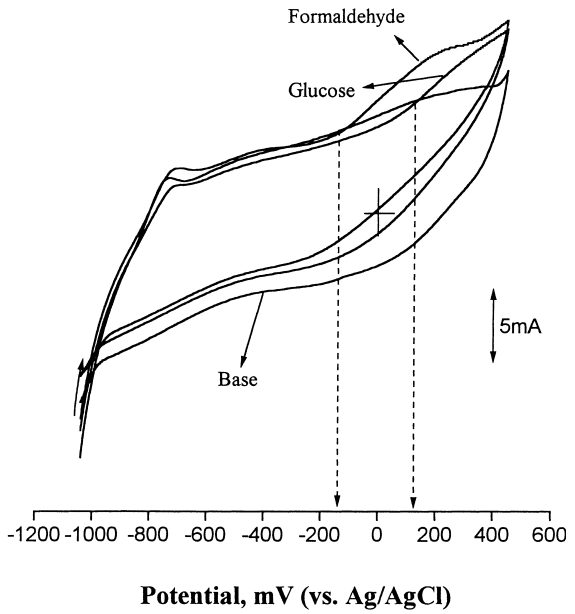

Fig. 2. Cyclic voltammograms for the electrocatalytic oxidation of formaldehyde and glucose (0.5 mM) on the PPCE in 1.1 M KOH solution at $v = 50$ mV/s.

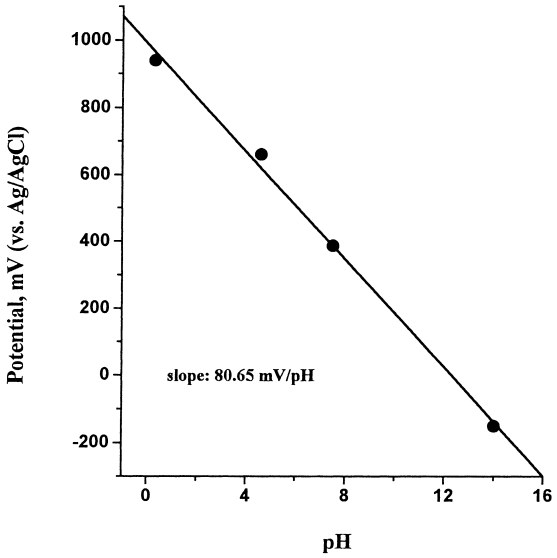

Fig. 3. Effect of solution pH on the anodic potentials of $Ru^{4+/6+}$ redox couple in the PPCE for formaldehyde oxidation reaction.

commences at −0.10 and 0.10 V versus Ag/AgCl (i.e. 1.12 and 1.32 V versus RHE), respectively. Interestingly, the obtained oxidation potentials lie exactly in the regions where $Ru^{4+/6+}$ and $Ru^{6+/7+}$ redox transitions occur. Furthermore, the glucose oxidation can be observed only in strong alkaline solution; whereas, the formaldehyde in all pHs. The difference is due to the absence of the $Ru^{6+/7+}$ state in lower pHs as mentioned earlier. Fig. 3 shows the pH-dependent redox potential of the $Ru^{4+/6+}$ redox transition for the formaldehyde oxidation at the PPCE. The starting oxidation potentials were taken as the redox potentials due to the very poor CV behavior. The measured redox potentials were found to decrease linearly with increasing in pH. Related experiments in the absence of formaldehyde confirmed the downward drift of peak potentials with the increase in pH. The slope of −80.65 mV/pH, rather than the Nernstian −59 mV/pH for pure RuO_2 electrodes [22,29,31], indicates the involvement of non-integral or fractional values in e^- and H^+ (or OH^-) [22,31]. Similar value of −75 mV/decade was observed for RuO_2/PVC paste electrode for the $Ru^{3+/4+}$ and $Ru^{4+/6+}$ redox transitions [31]. It is therefore expected that the redox reactions could occur due to the existence of polymeric or interlined products on the $Pb_2Ru_{1.75}Pb_{0.25}O_{7-y}$

surface and the number of H^+ or OH^- exchange with electrons is in non-stoichiometric ratios. Again, the results agree well with that of RuO_2 electrodes.

3.2. Interfacial surface charge analysis

In order to understand the electrochemical interfacial behavior in terms of accessible surface sites and to know about H^+ or OH^- coupled redox mechanism, scan rate variations were recorded on the PPCE in different pH solutions. Fig. 4A shows the typical CV response of the PPCE at different scan rates in 1 M H_2SO_4 solution. In all the scan rates, the obtained redox peak currents were very low with huge background currents. Therefore, instead of measuring current values, surface charges were taken as an estimating parameter to study the surface behavior of the PPCE. Voltammetric surface charges (q^*) were calculated from the integral area under the cyclic voltammograms. Since the charge during a voltammetric curves arised both by the non-faradic and faradic processes [28,29,31–33], the CV analysis of the PPCE indicated that the swallow of faradic contribution by non-faradic processes. Fig. 4B shows the typical plot of q^* versus v for the PPCE in different pH solutions. As can be seen, for all pH solutions, higher amount of q^* were observed at lower scan rates and it decreases with increase in scan rate. Trasatti and coworkers have done extensive work on this aspect for Ti/RuO_2 and they suggest that the rate of charging and discharging be limited by the diffusion of proton to the interfacial site of the oxide molecule [28,32,33]. The same explanation can also be applied to $Pb_2Ru_{1.75}Pb_{0.25}O_{7-y}$, and interestingly, the cathodic charge was about 15% higher than that of anodic one for the $Pb_2Ru_{1.75}Pb_{0.25}O_{7-y}$. This indicates that the penetration of OH^- (or ejection of H^+) during the anodic cycle is less favorable than the penetration of H^+ (or ejection of OH^-). For thermally prepared RuO_2, it was reported that the cathodic charge in chronopentiometric experiments is either about 50 or 30% lower than the charge extracted on the anodic process with a trend that is opposite to $Pb_2Ru_{1.75}Pb_{0.25}O_{7-y}$ [36,37]. This asymmetric in voltammetric charge may due to the existence of active oxygen species (O′) bonded to the Pb ion in the $Pb_2Ru_{1.75}Pb_{0.25}O_{7-y}$ molecule. During the anodic scan, the ejection of proton from the active O′ site is very difficult. On the other hand, because of the electrostatic attraction of H^+ species with active O′, the insertion of H^+ in the cathodic scan is more favorable.

Trassatti's surface formalism was also adopted in the present investigation to analyze the contribution of the interfacial surface charge [32]. The behavior that surface charges depend on the scan rate indicates the existence of different type of accessible species in $Pb_2Ru_{1.75}Pb_{0.25}O_{7-y}$, which may cause different H^+ (or OH^-) diffusion with scan rates [28,32,33]. Usually, the H^+ (or OH^-) prefers to diffuse on grain boundaries, such as pores, crevices, and cracks, than directly on the crystallite site [28,29,31]. The initial sharp decrease with scan rate is due to the existence of less accessible surface regions, which are accessible for proton exchange only at low scan rates. In other words, there is a fraction of available surface sites (i.e. proton-donating surface species), which are more difficult to exchange protons and thus become a rate determination step in particularly hidden surface regions.

The total voltammetric charge (q^*_{tot}), which is related to whole active surface, comes from two sources: (1) (q^*_{in}), charges related to the "inner" or less accessible surface regions including loose grain boundaries, pores, cracks, etc. (2) (q^*_{out}), charges related to the "outer" or more accessible surface regions where the redox reactions can occur without hindrance. It has been shown that the experimentally measured charge at different v, i.e. q^*_v, can be linearized if $(1/q^*_v)$ is plotted against $v^{1/2}$. The linear extrapolation to $v \to 0$ gives q^*_0, which is equal to q^*_{tot}, the surface charge density related to infinitely slow proton exchange [31,32]. The related surface charge thus measures the whole oxide surface wetted by the solution.

$$\left(\frac{1}{q^*_v}\right) = \left(\frac{1}{q^*_0}\right) + a(v^{1/2}) \tag{5}$$

$$q^*_0 = q^*_{tot} \qquad \text{at } v \to 0 \tag{6}$$

On the other hand, a plot of q^*_v versus $1/v^{1/2}$ at $v \to \infty$ give an intercept of q^*_{out}, which represents the amount of charge density related to the outer surface of the oxide that is accessible to proton exchange.

$$q^*_v = q^*_\infty + b\left(\frac{1}{v^{1/2}}\right) \tag{7}$$

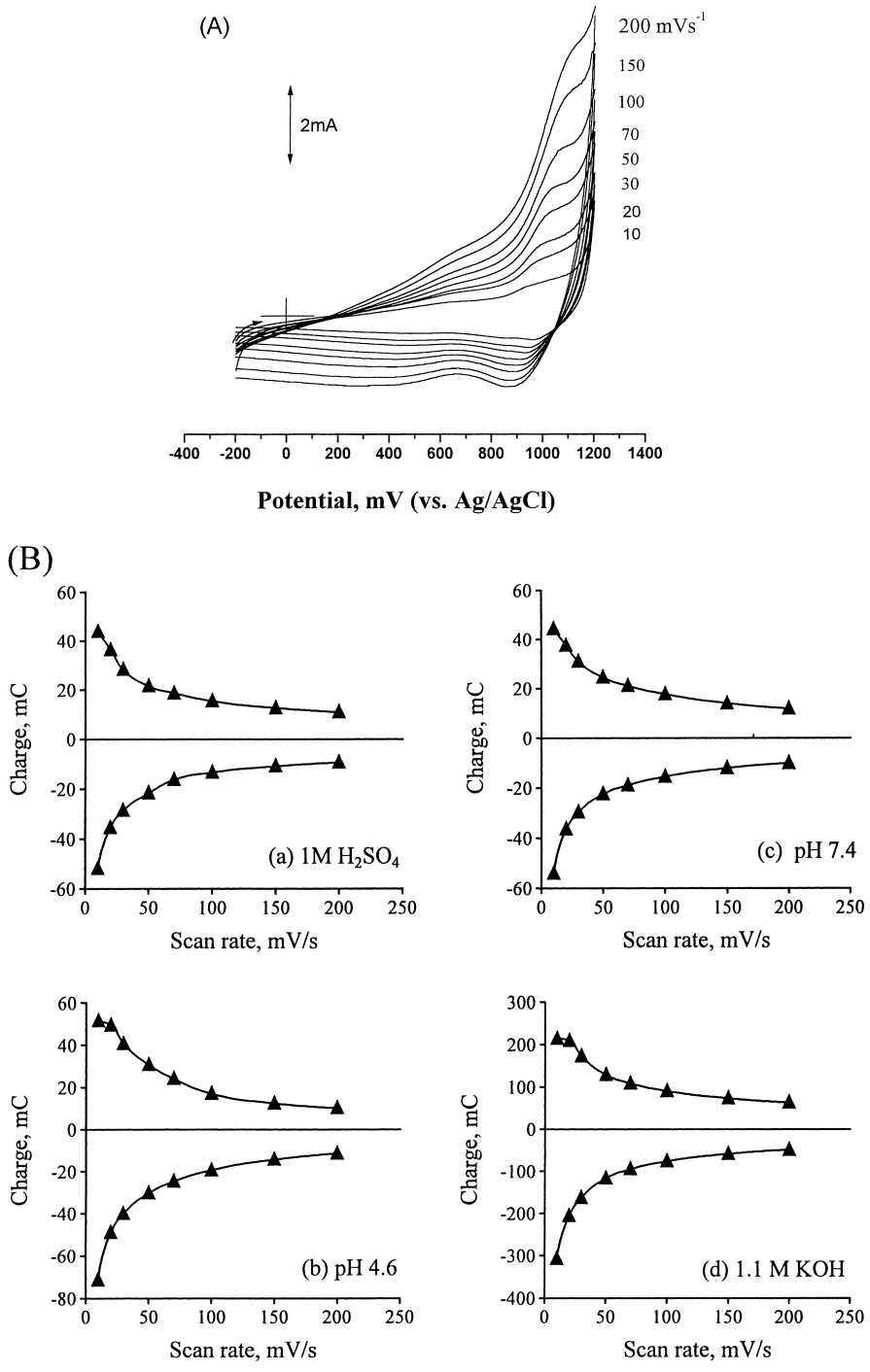

Fig. 4. (A) CV response of the PPCE in 1 M H_2SO_4 at various scan rates; (B) variation of voltammetric charge against scan rate for the PPCE at different solution pHs.

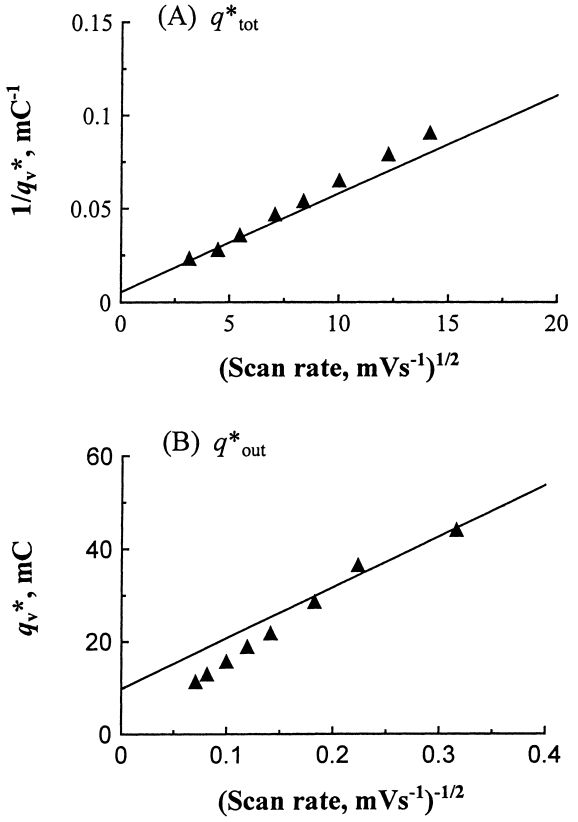

Fig. 5. Calculation of (A) q^*_{tot} and (B) q^*_{out} surface charge values for the PPCE in 1 M H_2SO_4 solution.

$$q^*_\infty = q^*_{out} \qquad \text{at } v \to \infty \tag{8}$$

Once q^*_{tot} and q^*_{out} are obtained, q^*_{in} is then calculated from $q^*_{tot} = q^*_{out} + q^*_{in}$. Typical linearized plots for the estimation of q^*_{tot} and q^*_{out} were given in Fig. 5 for the PPCE in 1 M H_2SO_4 solution. Estimated inner and outer charge components in 1 M H_2SO_4 and at other pH solutions are shown in Fig. 6. As can be seen, the q^*_{in} shared a major contribution to q^*_{tot} and reaches a maximum in 1.1 M KOH. The q^*_{out}/q^*_{in} ratio was found to decrease considerably with increasing in pH and is close to unity in alkaline solution. For RuO_2, the q^*_{out}/q^*_{in} ratio was reported as unity in all pHs indicating that the inner surface is about the same magnitude as the outer surface [32,33]. It is concluded that the $Pb_2Ru_{1.75}Pb_{0.25}O_{7-y}$ shows similar behavior to that of RuO_2 only in alkaline solution; whereas, the similarity decrease with decreasing in pH.

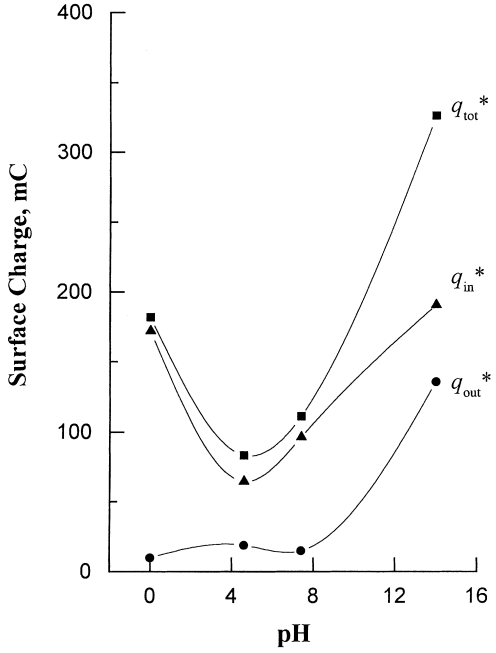

Fig. 6. Variation of q^*_{tot}, q^*_{in}, and q^*_{out} of the PPCE with solution pH.

A q^*_{tot} versus pH plot in Fig. 6 shows high charge values at extreme pHs and approximately four times lower charge value at intermediate pH. Most important of all, the pH where the minimum in the voltammetric charge occurred coincides with the pH_{PZC} of 3.9 measured from conventional titrimetic method for $Pb_2Ru_{1.75}Pb_{0.25}O_{7-y}$ [4]. The decrease in the voltammetric charge in solutions of intermediate pH is probably due to the poor dissociation effect of surface hydroxyl groups of the oxide material.

3.3. Catalytic reactions on $Pb_2Ru_{1.75}Pb_{0.25}O_{7-y}$ surfaces

For the catalytic reactions, the presence of higher oxidation species (either from Ru^{n+} or from Pb^{n+}) is expected to effectively participate in the catalytic mechanism. Previous report has already noticed the major contribution by ruthenium species in the octahedral sites of $Pb_2Ru_{2-x}Pb_xO_{7-y}$ [4,14]. Nevertheless, no insight view was provided regarding the electrochemical catalytic mechanisms with respect to that active higher oxidation ruthenium ion on the

$Pb_2Ru_{2-x}Pb_xO_{7-y}$ material. Unfortunately, it is impossible to perform catalytic studies on the PPCE due to the large double layer charging current. This problem, however, can be overcome by using a NPCE, which was prepared with a low oxide loading of 20 ppm in 4 wt.% Nafion solution. Because of the very low loading density, no redox peaks were noticed with these electrodes even in 1 M H_2SO_4 medium, and thus the catalytic signals can be easily observed with moderate concentration of analytes.

3.4. Electrocatalytic ORR on the NPCE

Because of the superior catalytic behavior towards the reduction reaction, $Pb_2Ru_{2-x}Pb_xO_{7-y}$ materials were previously used in fuel cell applications as ORR catalyst [4]. Our group further reported a novel in situ preparation procedure for preparing $Pb_2Ru_{2-x}Pb_xO_{7-y}$ in Nafion membrane by ion-exchange method (designated as NCME), and extend its usage for analytical detection of dissolved oxygen in aqueous solution [6–13]. Earlier, electrochemical polarization studies towards the ORR were also been studied both in acid and alkaline medium [17]. The mechanism was explained in terms of ruthenium species in a manner analogous to that of cleavage of carbon–carbon double bond with osmium or ruthenium tetraoxide. In the above mechanisms, the coordination number and number of sites of ruthenium is unclear. Later Goodenough et al. [14] studied the ORR in a wide range of pH by means of polarization method and results were well interpreted with pH_{PZC} and surface charge effect. Specifically, the mechanism was explained in terms of Ru^{3+} species. However, no solid evidence was provided about the Ru^{3+} participation and no mechanistic parameters were derived from the ORR on the $Pb_2Ru_{2-x}Pb_xO_{7-y}$ electrode. The main purpose of the present investigation is therefore to prove the mediation of Ru^{3+}, estimate the possible kinetic parameters, and derive the possible reaction mechanism for the ORR.

Fig. 7A shows the voltammetric behaviors of the NPCE in 1.1 M KOH solution without deaeration. As can be seen, the $E_{1/2}$ of ORR occurred at the potential window around −0.40 to −0.75 V versus Ag/AgCl (i.e. ∼0.47–0.82 V versus RHE) in the cathodic reverse scans. Interestingly, the magnitude of

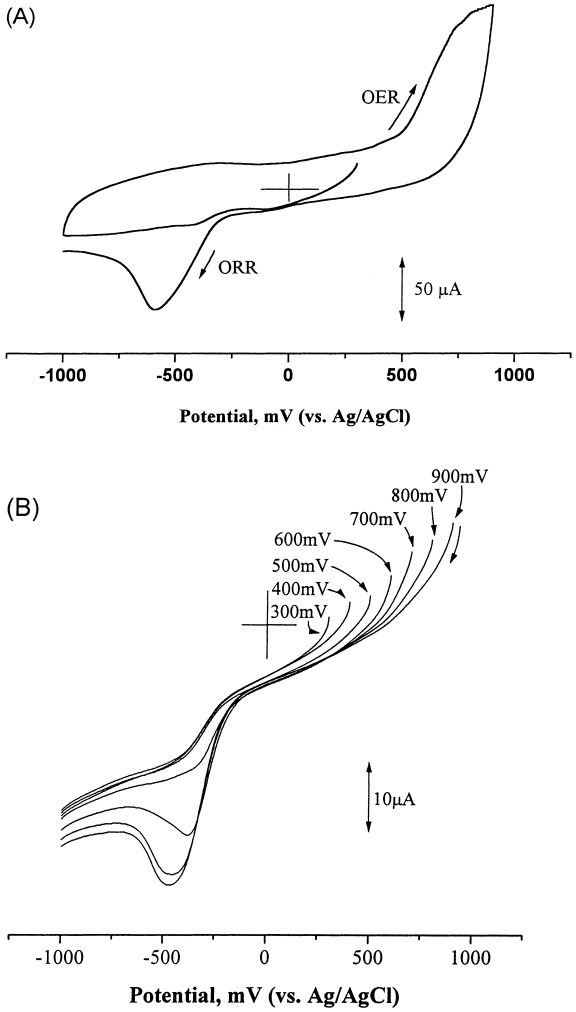

Fig. 7. (A) CV behavior of the NPCE at $v = 50$ mV/s in 1.1 M KOH solution; (B) the effect of holding potential (holding time = 15 s) to the ORR.

the ORR peak current depends on the holding potential in the OER region as shown in Fig. 7B. Note that the $Ru^{4+/3+}$ transition commences at ∼0.40–0.50 V versus RHE (based on Eq. (2)) in pH 14 solution and the ORR current signals (in Fig. 7A and B) were noticed close that potentials. This result actually strongly supports the mediation of the ORR by $Ru^{3+/4+}$ redox transitions. The existence of active O′ atom and in turn possessing of higher cathodic charge on $Pb_2Ru_{1.75}Pb_{0.25}O_{7-y}$ obviously leads to superior electrocatalytic activity than that of RuO_2 towards the

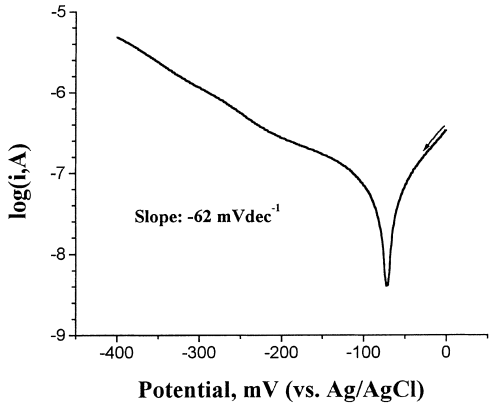

Fig. 8. Tafel plot for the ORR on the NPCE in 1.1 M KOH solution derived at $v = 1$ mV/s.

ORR. Indeed, only very few literatures were available regarding the ORR with RuO_2 [38].

In order to get more insight about the mechanistic aspects both steady-state polarization and RDE studies were made on the NPCE in alkaline solution. Fig. 8 shows the typical Tafel plot for the ORR in 1.1 KOH solution. The obtained Tafel slope ($-b_a = 2.303RT/F$), i.e. $(\partial E/\partial \log(i))_{pH}$, is ~60 mV/decade. The order of the overall reaction (m) can also be calculated by the method suggested earlier for OER on RuO_2 electrode [39,40]. In the present case, the calculated m for the ORR on the NPCE is ~1. Based on the b_a and m obtained, the possible mechanism can be derived as shown below in terms of *hydrogen peroxide path* [41].

$$O_2 + H_2O = O_2H_{ads} + OH_{ads} \quad (9)$$

$$O_2H_{ads} + H_2O \rightarrow O_2H_{2\,ads} + OH_{ads} \quad (10)$$

$$O_2H_{2\,ads} = 2OH_{ads} \quad (11)$$

$$OH_{ads} + e^- = OH^-_{ads} \quad (12)$$

In the above reactions sequence, the interaction between the surface adsorbed water molecule, i.e. O_2H_{ads} with that of solution water is considered to be a rate determining step, since it possess the Tafel slope of 60 mV with $m = 1$. Earlier Goodenoguh et al. reported the ORR mechanism based on the $Ru^{3+}O_tH$ species and assigned the chemical transfer of O_2^- to OH^- through $Ru^{3+}O_tH$ as the rate determination step without any kinetic support [14]. Here, we expect some positive interaction between the active O' species (which one may derived from faradic, i.e. $Ru^{4+/3+}$ process coupled with non-faradaic process like H^+ or OH^- diffusion) with that of O_2H_{ads} in the rate determination step to reduce the energy barrier on the ORR.

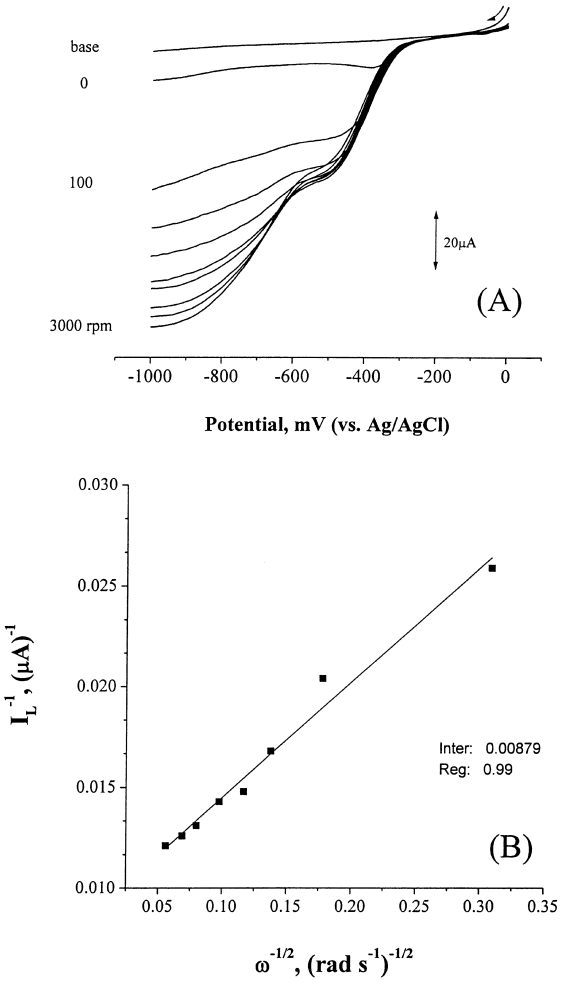

Fig. 9. (A) Typical RDE ORR response of the NPCE in 1.1 M KOH solution at different rpm's with $v = 2$ mV/s; (B) Koutecky–Levich plot for the data in (A).

RDE experiments concerns with ORR were also performed on the NPCE to calculate the heterogeneous rate constant value, k_h. Fig. 9A shows the RDE voltammetric response of the ORR in oxygen saturated alkaline solution. The obtained RDE response is not

regular. The current exhibits in two distinct regions, i.e. at −0.3 to −0.5 V and at −0.6 to −0.9 V versus Ag/AgCl with poorly defined plateau region. Similar types of RDE voltammograms were also noticed in the case of ORR in Zn surface [42]. The possible reasons were explained in terms of accompanying of radical path with sequential ORR mechanism, also supports the above said mechanism. Koutecky–Levich plot for the ORR has been plotted in Fig. 9B. Rate constant values for the ORR was estimated according to the following RDE equations.

$$\frac{1}{i_{\text{red}}} = \frac{1}{i_{\text{k}}} + \frac{i_{\text{red}}}{[(0.62nFC^{\text{b}}_{\text{red}}D^{2/3}_{\text{red}}v^{-1/6})\omega^{1/2}]}$$

$$i_{\text{k}} = nFAk_{\text{h}}C^{\text{b}}_{\text{red}} \tag{13}$$

where number of electrons, $n = 4$, oxygen bulk concentration, $C^{\text{b}}_{\text{red}} = 10^{-6}$ M [43], k_{h} is the heterogeneous rate constant, and other terms are its usual significance. The obtained mass transfer corrected current value (i_{k}) is 113.76 μA. Based on Eq. (13), the rate constant for the ORR is 4.17×10^{-3} cm^2/s. This rate constant value is comparable with that of earlier electrocatalytic results towards the ORR [42].

3.5. Electrocatalytic oxidation of dopamine on the NPCE

The RDE studies of dopamine oxidation on NPCE (Fig. 10A) shows the catalytic current signals in the potential window of 0.15–0.30 V versus Ag/AgCl (i.e. ∼0.44–0.59 V versus RHE) in pH 7 phosphate solution. Compared to GCE and to other earlier studies on the same topics [44,45], it was about 200–100 mV less in overpotential on the NPCE. The enhanced catalytic activity could also be certainly attributed to the participation of higher oxidation ruthenium species in the pyrochlore structure. Based on Eq. (2), with the consideration of $(\partial E/\partial \text{pH}) = -75$ mV/decade, the redox potential of $Ru^{4+/6+}$ in pH 7 phosphate buffer should lie between ∼0.24–0.34 V versus Ag/AgCl. Since the obtained catalytic activity of dopamine fall close in this potential window, it is clear that the $Ru^{4+/6+}$ present in the Ru_2O_6 octahedral sites of the pyrochlore structure mediate the catalytic oxidation of dopamine. Similar type of $Ru^{4+/6+}$ mediated electrocatalytic mechanism was also demonstrated

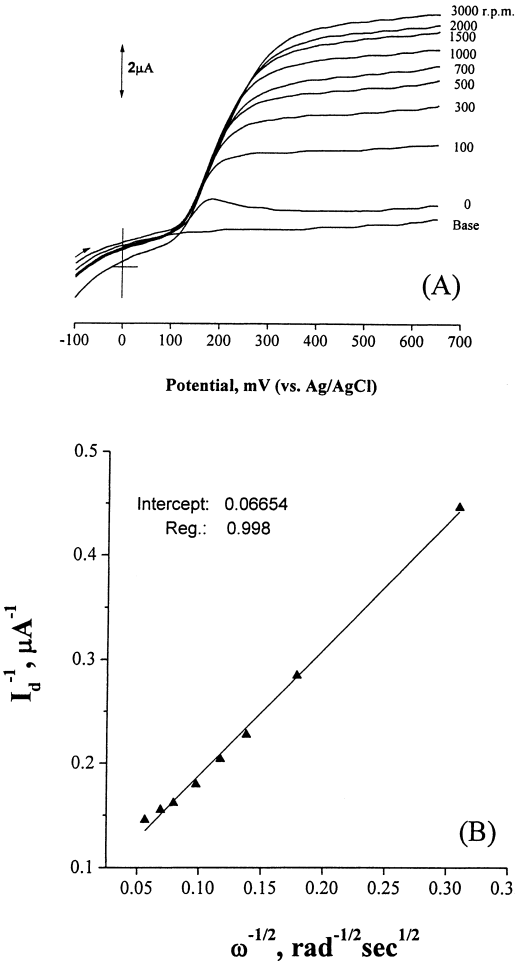

Fig. 10. (A) RDE response of 100 μM dopamine on the NPCE in pH 7.4 phosphate buffer at different rpm's with $v = 2$ mV/s; (B) Koutecky–Levich plot for the data in (A).

by our group for the cysteine oxidation reaction on the NCME [46]. Based on all these studies, the schematic picture of the ruthenium mediated oxidation mechanism for dopamine on NPME is shown in Scheme 1.

Kinetic analyses were done using the RDE technique and typical RDE response of 100 μM dopamine in pH 7.0 phosphate buffer at $v = 2$ mV/s is given in Fig. 10A. Perfect sigmoid limiting current responses were noticed on all rpm's. Mass transfer corrected current value, i_{k}, was calculated to be 15.029 μA from the Koutecky–Levich plot (Fig. 10B). The calculated

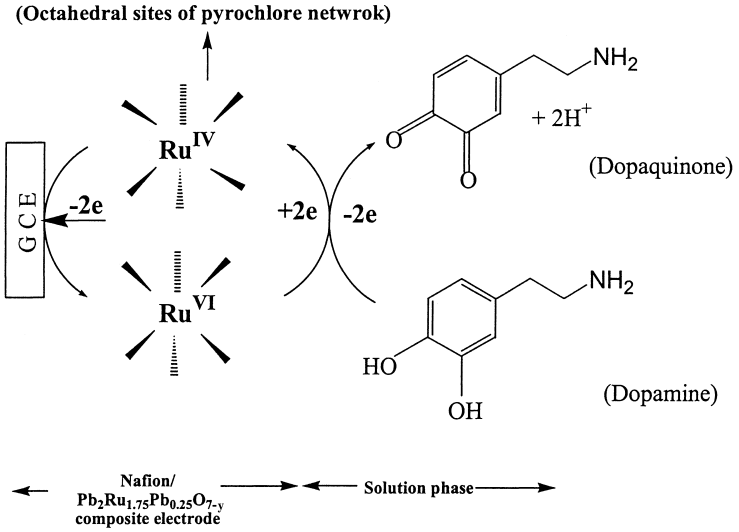

Scheme 1. Electrocatalytic mediated mechanism for dopamine oxidation on the NPCE.

heterogeneous rate constant value (k_h) for the dopamine oxidation reaction is 11.02×10^{-3} cm^2/s.

4. Conclusions

The following conclusions can be summarized from this study:

1. The cyclic voltammetric analysis on the PPCE showed redox behavior with predominant effect similar to that of RuO_2.
2. Based on the formaldehyde and glucose oxidation reaction on the PPCE and ORR on the NPCE, the possible ruthenium redox species exist in the catalyst are $Ru^{3+/4+}$, $Ru^{4+/6+}$, and $Ru^{6+/7+}$. The redox transition of $Ru^{6+/7+}$ is only available at pH $>$ 12.
3. The redox potential of the formaldehyde oxidation on the PPCE is pH-dependent with $\partial E/\partial$pH close to -80 mV/decade. The operation of non-Nernstian behavior is due to the existence of polymeric and interlined surface oxide in $Pb_2Ru_{1.75}Pb_{0.25}O_{7-y}$.
4. The fact that the surface charge is scan rate-dependent indicates the presence of different types of accessible species with H^+ or OH^- through diffusion on the surface sites of $Pb_2Ru_{1.75}Pb_{0.25}O_{7-y}$. The cathodic charges were 15% higher than anodic charges in varied scan rates at all pHs; while, it is reverse in the case of RuO_2. This property and the presence of active O′ species make $Pb_2Ru_{1.75}Pb_{0.25}O_{7-y}$ a better catalyst than RuO_2 in the ORR.
5. The q^*_{out}/q^*_{in} ratio is almost unity in alkaline solution and decreases with increasing in pH; while, it is almost unity in all pHs for RuO_2. This result suggests that $Pb_2Ru_{1.75}Pb_{0.25}O_{7-y}$ has similar behavior to that of RuO_2 only in alkaline solution; whereas, the similarity decrease with decreasing in pH.
6. The obtained pH_{PZC} of 3.9 from electrochemical experiment matches exactly with the titrimetric value revealing the reliability of the present experiments.
7. The electrocatalytic mediated ORR and dopamine oxidation on the NPCE confirms the mediation of ruthenium species present in the Ru_2O_6 octahedral site of $Pb_2Ru_{1.75}Pb_{0.25}O_{7-y}$. The superior electrocatalytic response of $Pb_2Ru_{1.75}Pb_{0.25}O_{7-y}$ than that of RuO_2 towards the ORR is due to the surface charge effect.

Acknowledgements

The authors gratefully acknowledge financial support from the National Science Council of the Republic of China.

References

[1] S. Trasatti, G. Lodi, in: S. Trasatti (Ed.), Electrodes of Conductive Metal Oxides, Part A, Elsevier, New York, 1981, p. 301.
[2] K. Chandrasekara Pillai, A. Senthil Kumar, J.-M. Zen, J. Mol. Catal. A 160 (2000) 277.
[3] M.E.G. Lyons, in: I. Prigogine, S.A. Rice (Eds.), Advances in Chemical Physics, Wiley, New York, 1996, p. 297.
[4] J.-M. Zen, R. Manoharan, J.B. Goodenough, J. Appl. Electrochem. 22 (1992) 140.
[5] L. Swette, J. Giner, J. Power Sources 22 (1988) 399.
[6] J.-M. Zen, C.-B. Wang, J. Electroanal. Chem. 368 (1994) 251.
[7] A.M. Kannan, A.K. Shukla, S. Sathyanarayana, J. Electroanal. Chem. 281 (1990) 339.
[8] J.A.R. van Veen, J.M. van der Eijk, R. de Ruiter, S. Huizinga, Electrochim. Acta 33 (1988) 51.
[9] J.-M. Zen, J.-S. Tang, Anal. Chem. 67 (1995) 208.
[10] J.-M. Zen, J.-S. Tang, Anal. Chem. 67 (1995) 1892.
[11] J.-M. Zen, Y.-S. Ting, Anal. Chim. Acta 342 (1997) 175.
[12] J.-M. Zen, I.-L. Chen, Electroanalysis 9 (1997) 9.
[13] J.-M. Zen, Y.-S. Ting, Y. Shih, Analyst 123 (1998) 1145.
[14] J.B. Goodenough, R. Manoharan, M. Paranthaman, J. Am. Chem. Soc. 112 (1990) 2076.
[15] J.M. Longo, P.M. Raccah, J.B. Goodenough, Mater. Res. Bull. 4 (1969) 191.
[16] R. Manoharan, M. Paranthaman, J.B. Goodenough, Eur. J. Solid State Inorg. Chem. 26 (1989) 155.
[17] H.S. Horowitz, J.M. Longo, H.H. Horowitz, J. Electrochem. Soc. 130 (1983) 1851.
[18] G. Gokagac, B.J. Kennedy, J. Electroanal. Chem. 353 (1993) 71.
[19] G. Gokagac, B.J. Kennedy, J. Electroanal. Chem. 368 (1994) 235.
[20] D. Galizzioli, F. Tantardini, S. Trasatti, J. Appl. Electrochem. 4 (1974) 57.
[21] L.D. Burke, O.J. Murphy, J.F. O'Neil, S. Venkatesan, J. Chem. Soc., Faraday Trans. 1 73 (1977) 1649.
[22] L.D. Burke, J.F. Healy, J. Electroanal. Chem. 124 (1981) 327.
[23] L.D. Burke, M.E.G. Lyons, E.J.M. O'Sullivan, D.P. Whelan, J. Electroanal. Chem. 122 (1981) 103.
[24] S. Trasatti, G. Lodi, in: S. Trasatti (Ed.), Electrodes of Conductive Metal Oxides, Part B, Elsevier, New York, 1981, p. 521.
[25] M.E.G. Lyons, L.D. Burke, J. Chem. Soc., Faraday Trans. 1 83 (1987) 299.
[26] E.J. O'Sullivan, E.J. Calvo, in: R.G. Compton (Ed.), Chemical Kinetics, Vol. 27, Elsevier, Amsterdam, 1987, p. 247.
[27] G.W. Jang, E.W. Tsai, K. Rajeshwar, J. Electroanal. Chem. 263 (1989) 135.
[28] S. Trasatti, in: J. Lipkowski, P.N. Ross (Eds.), Electrochemistry of Novel Materials, VCH Publishers, 1995.
[29] A.S. Kumar, Ph.D. thesis, A.C. College of Technology, University of Madras, Madras, 1998.
[30] D.W. Lam, K.E. Johnson, D.G. Lee, J. Electrochem. Soc. 125 (1978) 1069.
[31] A. Senthil Kumar, K. Chandrasekara Pillai, J. Solid State Electrochem 4 (2000) 408.
[32] S. Aridizzone, C. Fregonara, S. Trasatti, Electrochim. Acta 35 (1990) 263.
[33] M. Kodintsev, S. Trasatti, M. Rubel, A. Wiecekowski, N. Kaufher, Langumuir 8 (1992) 283.
[34] E.J.M. O'Sulivan, J.R. White, J. Electrochem. Soc. 136 (1989) 2576.
[35] M.E.G. Lyons, C.A. Fitzgerald, M.R. Smyth, Analyst 119 (1994) 855.
[36] G. Lodi, G. Zucchini, A. DeBattistie, E. Siveri, S. Trasatti, Mat. Chem. 3 (1978) 179.
[37] J.E. Weston, B.C.H. Steele, J. Appl. Electrochem. 10 (1980) 49.
[38] C.-C. Chang, T.-C. Wen, J. Appl. Electrochem. 27 (1997) 355.
[39] A. Damjanovic, J. Electrochem. Soc. 138 (1991) 2315.
[40] L.I. Krishtalik, Electrochim. Acta 26 (1981) 329.
[41] K.C. Pillai, J.O'M. Bockris, J. Electrochem. Soc. 131 (1984) 568.
[42] H.S. Wroblowa, S.B. Qaderi, J. Electroanal. Chem. 295 (1990) 153.
[43] R.E. Davis, G.L. Horwath, C.W. Tobias, Electrochim. Acta 12 (1967) 287.
[44] G.A. Rivas, V.M. Solis, Anal. Chem. 63 (1991) 2762.
[45] R.B. Kawde, N.B. Laxmeshwar, K.S.V. Santhanam, Bioelectro. Bioener. 34 (1994) 83.
[46] J.-M. Zen, A. Senthil Kumar, J.-C. Chen, Chem. Lett. 8 (1999) 743.